2022

Mathematical Model for the Mechanical Losses and Validation Experiments

Atacan Oral

Ismail Lazoglu

Husnu Kerpicci

Seckin Tuysuz

Mathematical Model for the Mechanical Losses and Validation Experiments

Atacan ORAL[a] , Ismail LAZOGLU [a]*, Hüsnü KERPİÇÇİ[b], Seçkin TÜYSÜZ[b]

[a]Manufacturing and Automation Research Center, Koc University, Istanbul, Turkey.
[b]Arcelik A.S. Central R&D, Istanbul, Turkey.
aoral18@ku.edu.tr, ilazoglu@ku.edu.tr, husnu.kerpicci@arcelik.com, seckin.tuysuz@arcelik.com

* Corresponding Author

ABSTRACT

Energy consumption is one of the hot topics nowadays in almost every industry. Reciprocating compressors that are installed in household refrigerators contain various energy consumption sources. Along with the thermodynamics and electronic component-based losses, there are also mechanical losses due to frictional forces in reciprocating compressors. These frictional forces emerge on the piston-cylinder translational bearing, journal bearings and thrust bearing. In this study, a mathematical torque prediction model is established for the steady-state operation where piston-cylinder contact model is developed by following the work of Greenwood and Tripp, which considers contact mechanics. In contrast, journal bearing frictions are estimated based on Newton's viscosity principle and thrust bearing torques are predicted by simply calculating the torque generated on the surface by crankshaft due to its mass. In addition, a mechanical loss measurement setup has been established where the compressor is driven externally with the help of an eccentric rod that is mounted on the top of the crankshaft. Experimental torque measurements have been made according to the torsional behavior of the rod that acts as a bridge between the external motor and the crankshaft. The theoretically predicted torque and loss values have been validated with experimental data. A comparison between the previous and new mechanical loss measurement setup has also been made and repeatability, as well as reliability of the new measurement method, was observed.

1. INTRODUCTION

Among other domestic appliances, household refrigerators are considered as one of the major energy consumers worldwide due to their uninterrupted operation to preserve food items. Therefore, improving the energy efficiency of domestic refrigerators is of key importance nowadays. The primary source of energy consumption in a domestic refrigerator is the compressor, which comprises a crankshaft coupled with an electric motor. The presence of frictional forces between different moving parts of the compressor significantly degrades the performance and increases the overall energy expenditure. A reciprocating compressor contains three primary friction force sources: forces on journal bearing due to crankshaft rotation, forces on piston-cylinder contact due to translation and secondary motion of the piston, and frictional forces on thrust bearing due to mass of rotating crankshaft.

There are both numerical and experimental approaches to determine frictional losses. Posch et al. (2016) reported a numerical analysis in which the Reynolds equation integrated multibody dynamics formulations are utilized to predict losses on journal bearing, Mantri et al. (2014) utilized Reynold's equation via finite-difference modeling to result in pressure distribution, forces and power loss on piston-cylinder contact.

This study estimates mechanical losses due to friction forces on piston-cylinder contact, journal, and thrust bearing. Afterward, the estimations were validated with a recently established experimental setup.

In order to measure the mechanical losses, an experimental setup similar to the work of Rao et al. (1996) was established where the compressor is fixed into housing and driven externally. A torque meter was located in between the crankshaft and the external motor to record the torsion produced by the motor excitation and friction forces on the torque meter's rods. Afterward, torque values were multiplied with the angular velocity of the crankshaft to predict mechanical losses.

2. MATERIALS AND METHOD

2.1 Theoretical Calculations

To obtain the mechanical loss values of the compressor due to frictional forces, each component must be investigated individually. Therefore, first friction forces on piston-cylinder contact are analyzed, then forces on journal bearing and thrust bearing are included. By multiplying the forces with the object's path, the work of the friction force can be obtained. Furthermore, the losses can also be found by multiplying the emerging torques with the constant angular velocity.

2.1.1 Piston Cylinder Forces

Friction force due to the piston's reciprocation is a combination of lubricant oil shear and contact of asperities of the surfaces. It is a function of crank angle, piston length, piston diameter, lubricant shear pressure, friction coefficient, contact pressure and velocity of slider/piston. Secondary motion is omitted for piston and crankshaft in this study. Oil film thickness is assumed constant and hydrodynamic pressure variation along with the piston surface is neglected. Also, it is assumed that no waviness exists on piston and cylinder surfaces. Finally, the effect of gas force is excluded.

The friction force that occurs due to the piston movement is defined in Eq. 1 (Patir and Cheng, 1978, Gunelsu and Akalin, 2014).

$$F_f = -sign(U) \int_0^L \int_0^{2\pi} (p_{ls} + \mu_f p_c)\, d\alpha dz \qquad (1)$$

where U is the velocity of piston, yet the signum function only considers the direction of velocity. L is introduced as the length of piston, p_{ls} is lubricant shear pressure on piston, μ_f is friction coefficient and p_c is the contact pressure between solid-solid surfaces i.e. asperities. The variables are demonstrated in figure 1.

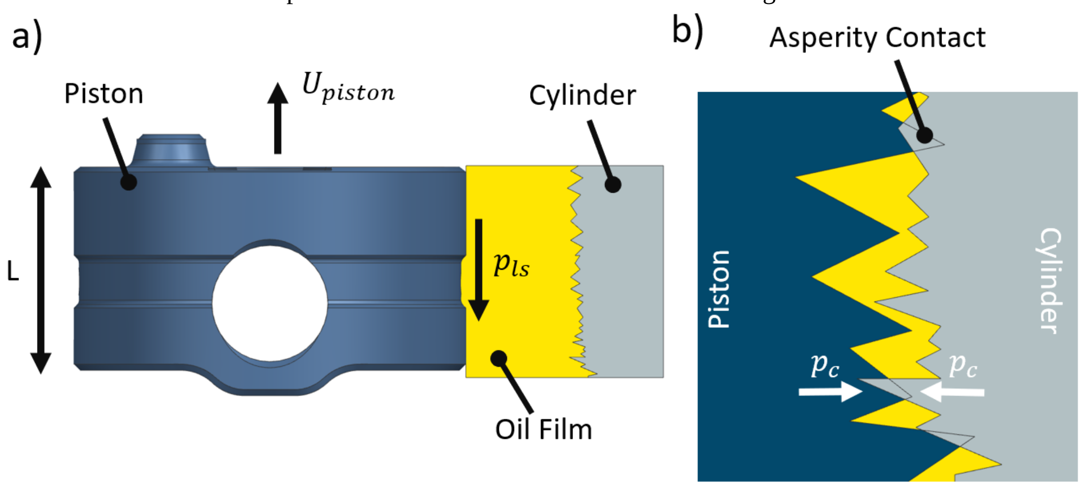

Figure 1. (a) Piston and lubrication film, (b) asperity contact in case of unsatisfactory oil supply

Greenwood and Williamson (1966) defined a statistical type of contact model (Jedynak and Gilewicz, 2013) that claims the interaction between two rough surfaces can be modelled by contact between an equivalent single rough surface and a flat surface. It is assumed that rough surfaces contain asperities that have spherical summits. It is also claimed that all asperity summits have same the radius β' but their heights vary randomly.

Furthermore, in case of contact between two surfaces, while some of the asperities plastically and elastically deform, asperities with relatively shorter height remain their shape. Greenwood and Tripp (1971) declared that while the height of a particular asperity is random, the distribution of their heights is rather close to Gaussian distribution.

In addition, average contact pressure is expressed as;

$$p_c = KE'F_{2.5}(H_\sigma) \tag{2}$$

$$K = \frac{8\sqrt{2}}{15}\pi(X\beta'\sigma)\sqrt{\frac{\sigma}{\beta'}} \tag{3}$$

where N is number of asperities per unit contact area, E' is composite modulus of elasticity and the function $F_{2.5}(H_\sigma)$ relates the probability distribution of asperity height i.e. rough surface with Gaussian distributed asperities (Hu et. al., 1994).

$$E' = \frac{2}{\left(\frac{1-v_1{}^2}{E_1}\right)+\left(\frac{1-v_2{}^2}{E_2}\right)} \tag{4}$$

Probability distribution of asperity height is also given as;

$$F_{2.5}(H_\sigma) = \begin{cases} A(\Omega - H_\sigma)^Z & H_\sigma \le \Omega \\ 0 & H_\sigma > \Omega \end{cases} \tag{5}$$

The Ω is an assumed constant which is equal to 4. In addition, parameter H_σ is given as the ratio of oil film thickness over surface roughness.

$$H_\sigma = h/\sigma \tag{6}$$

where h is the oil film thickness.

Clearance between cylinder and piston is around 7 microns in diameter and roughness value of (Ra) a randomly selected surface of 1.2x0.9 mm was measured approximately as 300 nanometers with White Light Interferometer for the investigated compressor and experimental data is shared in figure 2.

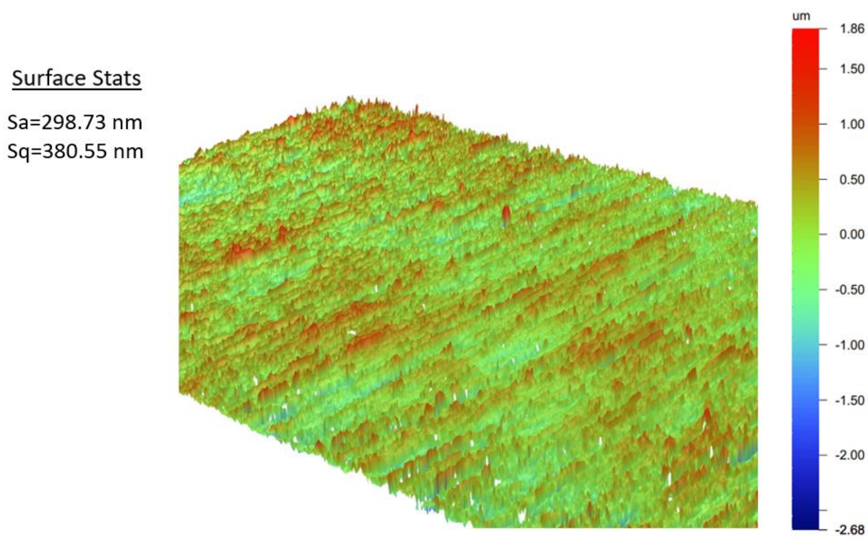

Figure 2. Measured surface of piston

While the heights of asperity values vary from 1.86 to -2.68 micrometer, where a negative value indicates a valley, the average roughness was measured as 288 nm.

In addition, as it is demonstrated in figure 3, asperity heights demonstrate a Gaussian distribution indeed.

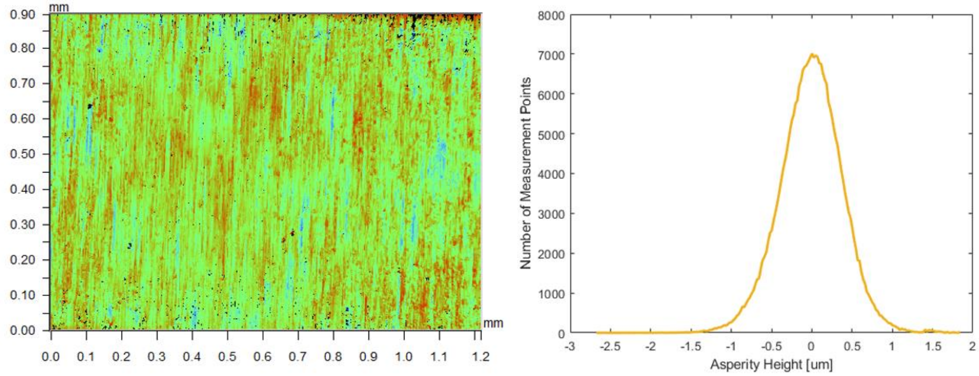

Figure 3. Gaussian distribution of asperities on the surface

Based on equation 5 and 6, it is safe to say that value of probability distribution of asperities can be assumed zero for the investigated components since the ratio of oil film thickness over surface roughness is larger than 4. Thus, the contact pressure is neglected in this study. In other words, the forces that emerged during piston reciprocation are carried by only the oil film during steady state, rather than asperities.
In such case, lubricant shear pressure acting on surface can be calculated as defined by Zhu et al. (1992).

$$\tau = -\frac{\mu U}{\bar{h}}\left(\Phi_f + \Phi_{fs}\right) + \Phi_{fp}\frac{\bar{h}}{2}\frac{\partial p_h}{\partial y} \tag{7}$$

Average shear stress factors, $\Phi_f, \Phi_{fs}, \Phi_{fp}$ are used to consider the surface waviness and roughness effects and shared at Eq. 8, 9, 10 for the case of zero waviness on the piston surface.

$$\Phi_f = \frac{h}{2\sigma}\ln\left(\frac{h+\sigma}{h-\sigma}\right) \tag{8}$$

$$\Phi_{fs} = \frac{3}{2}\left[\frac{h}{\sigma}\ \ln\left(\frac{h+\sigma}{h-\sigma}\right) - 2\right] \tag{9}$$

$$\Phi_{fp} = 1 - \left(\frac{\sigma}{h}\right)^2 \tag{10}$$

2.1.2 Journal Bearing Forces

Newton's viscosity law is utilized to estimate the friction forces on journal bearing due to crankshaft rotation (Jia, B., 2018).

$$\tau = \gamma\frac{U}{h} = \gamma\frac{2\pi r N}{c} \tag{11}$$

and force can be written as the multiplication of shear stress with surface area;

$$F = \tau A = \gamma\frac{2\pi r N}{c}2\pi r Z \tag{12}$$

where μ is viscosity, c is clearance. It is assumed that clearance is fully filled with oil as a pure uniform film and oil thickness is kept constant. Thus,

$$F \approx \pi D_b Z \gamma\left(\frac{\pi D_b N}{\bar{h}}\right) \tag{13}$$

where N is speed of crankshaft, $\bar{h}$ is clearance, Z and D_b are length and diameter of the bearing respectively.
While rpm is significantly affecting the force value, it is also worth mentioning that the effect of gas force on the losses is omitted and the tilting motion of crankshaft is excluded in the calculations. Viscosity of oil was obtained

based on the oil temperature that is measured during a detailed compressor temperature measurement experiment via thermocouples.
Since the investigated reciprocating compressor contains two journal bearings, the total length of the bearings must be used.

2.1.3 Thrust Bearing Forces

A simple approach that utilizes mass of crank as a load that is created on a surface was employed to estimate frictional forces on the thrust bearing (Nagata et al, 2012).

$$T = \int_A^0 dT = \int_A^0 \mu_k F r dA \tag{14}$$

and

$$T = \mu_k \left(\frac{F}{\pi(R_0^2 - R_1^2)}\right) \int_{R_1}^{R_0} r\, 2\pi r\, dr \tag{15}$$

Thus;

$$T = \frac{2}{3}\mu_k F \left(\frac{R_0^3 - R_1^3}{R_0^2 - R_1^2}\right) \tag{16}$$

where μ_k is friction coefficient between cast iron-cast iron material couple in an environment where oil exists (Barrett, 1990), F is the force generated due to the mass of crankshaft, R_0 and R_1 are the outer and inner contact diameters of the thrust bearing as depicted in figure 4.

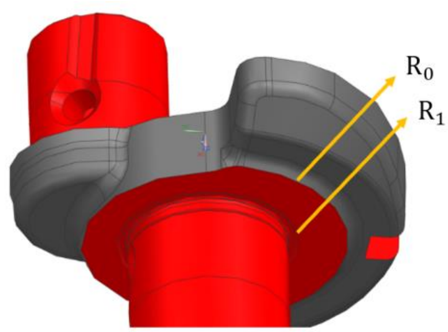

Figure 4. Inner and outer diameter of thrust bearing

2.2 Experimental Setup

The crankshaft's deceleration and inertia were being utilized in a previous experimental setup (Kerpicci et al., 2019) in such a way that a gear and clutch mechanism which is connected to the crankshaft is removed after the compressor reaches steady state rpm. Afterward, by considering angular velocity and angular deceleration of the shaft, friction work was being obtained.
Such method was altered since additional instruments such as gear and clutch were required. Therefore, an experimental setup that simulates real life more successfully was established where the compressor is separated from springs as well as discharge tube and fixed on a specially designed fixture. The compressor was excited with an external motor, the motion was transmitted from motor to the compressor with the help of couplings. An eccentric rod was utilized to eliminate the eccentricity of crankshaft rotation axis and crank-conrod bearing and it was mounted on the top surface of the shaft as a bridge to the coupling. A torquemeter was placed in between compressor and the motor in a way that it measures the torsion difference, $\theta_1 - \theta_2$, due to friction forces of the compressor and excitation of motor.

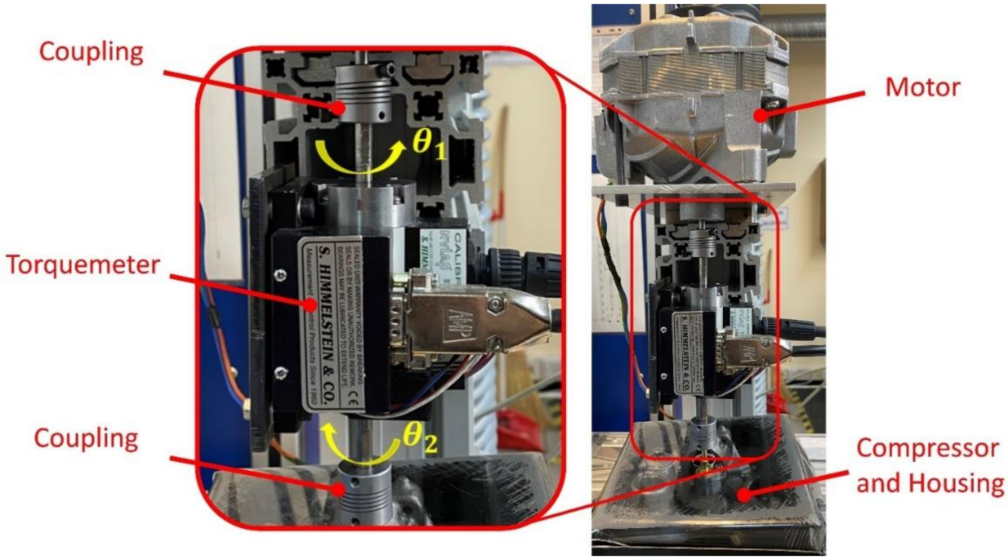

Figure 5. Experimental setup

Oil temperatures in steady-state operation for various rpms were acquired from the tests that are conducted in a calorimeter via thermocouples. In order to simulate the working condition temperatures in household applications, a heater with a feedback loop was placed underneath the housing of the compressor to control and to increase the temperature of oil to steady-state temperature level. Thanks to the feedback control algorithm, the temperature of the oil was kept at the desired level throughout the experiments. In order to preserve the oil inside the housing, a plastic plate was attached on top of the housing. Five thermocouples were utilized in the experimental setup to measure the temperature of the oil as well as compressor body. While four thermocouples were placed at the corners of the housing inside the oil, the last one was attached into a hole on the body near to the cylinder. Once the temperature balance was achieved, measurements were conducted for one minute and repeated four times. Afterward, the average of four experiments was calculated as the torque value.

3. RESULTS

3.1 Theoretical Estimations and Experimental Validations

The sum of torques can be multiplied with the constant angular velocity to determine the mechanical losses of the whole compressor or losses from different components can be also obtained individually. By governing the Eq 1-9 from 0 to 360 degrees crankshaft angle, the friction forces can be predicted on piston-cylinder contact for one crank revolution values are given with respect to a reference variable f.

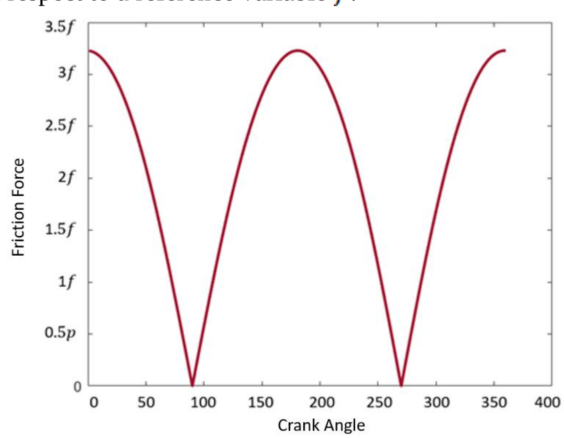

Figure *6*. Friction force versus crank angle

From figure 6, It can be seen that minimum friction force values were obtained at 0°, 180° and 360° i.e. at dead positions as expected since the piston dwells for an infinitesimal time period. Furthermore, at 90 and 270 degrees of crank angle, friction forces reach to maximum value due to the physical fact that crank pulls the piston towards thrust and antithrust regions, thus piston is exposed to more friction. By multiplying the friction force with the stroke of the piston in a cycle duration, the friction work, i.e. losses due to piston motion can be calculated. It is necessary to mention that secondary motion of the piston is omitted from the calculations. Also, in order to reflect the effect of both the lowest and the highest value of piston loss in one cycle of the crank, rms values were utilized.

In addition, since the aim is to obtain losses in steady state region, the rpm was also kept constant during a cycle in journal bearing loss calculations. The torque created by friction force of crank at the axis of rotation and torque that occurs on the thrust bearing due to the mass and rotation of the crankshaft were multiplied with angular velocity and utilized in loss predictions.

The total amount of mechanical losses was obtained by summing the individual losses on piston-cylinder, journal and thrust bearings by assuming that the losses remain the same in magnitude throughout steady state operation.

The experiments were started once the temperature values that were obtained through thermocouples were settled to the desired level. The tests were repeated four times for 60 seconds to consider repeatability and average torque values were recorded. Then, measured torque values were multiplied with angular velocity to end up with losses due to only friction forces. In addition, 10 cSt of oil was utilized in the experiments and the temperature of oil was controlled based on real life working condition for each rpm.

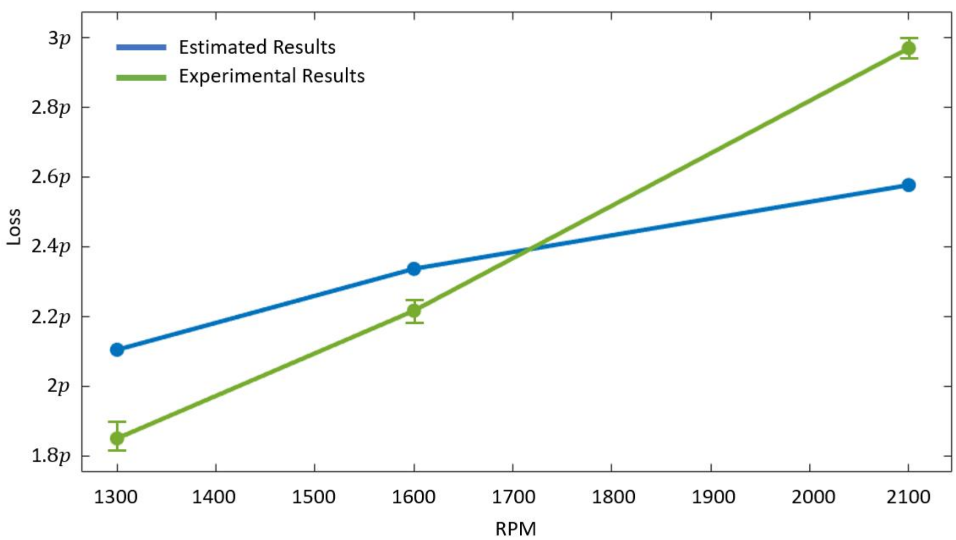

Figure 7. Experimental loss values vs estimated loss values

Figure 7 represents the theoretical calculations and experimental mechanical loss data, and values are given with respect to a reference variable p±0.2 W. It is safe to say that the repeatability condition is achieved for the experimental work. The percentage difference of experiments and calculations are 12%, %5 and %13 for 1300, 1600 and 2100 rpm, respectively. The change in difference can be explained by dynamics, secondary motion and friction mechanisms. While less side forces are expected at 1300 rpm in the moving mechanism, less secondary motion should also be observed. Yet, uniform oil film may not be accumulated. Since it is assumed that oil film surrounds the crankshaft as a pure homogenous film in calculations, the error difference in 1300 rpm condition is relatively higher than the case of 1600 rpm. In case of 1600 rpm, side forces are less than 2100 but oil distribution around the crank is achieved more successfully than 1300 rpm since it is known that as rpm increases better oil feed from the crank grooves is achieved. Therefore, excluding secondary motions do not affect the result significantly and the error difference in theoretical estimations is quite small. When the steady state rpm is 2100, even though oil suction from the oil pool is no longer an issue, side forces start to increase significantly. Therefore, the effect of secondary motion of both piston and crank plays a more active role in high speeds in experiments and the error value increases since secondary motions are omitted in calculations.

4. CONCLUSION

In this work, mechanical losses due to friction forces of a reciprocating compressor were investigated. Losses on piston cylinder bearing, journal bearing and thrust bearing were estimated with no-load condition, then validated with an experimental setup where the cylinder head, valves etc. were removed from the compressor. It was observed that theoretical estimations hold with an acceptable level of error margin with the experimental results, yet the calculations can be enhanced by including oil film thickness variation as well as secondary motion of piston and crankshaft tilting since both the phenomenon are introducing an additional motion axis to the system and forcing components to undesired friction.

NOMENCLATURE

F	force	(N)
U	piston velocity	(m/sec)
L	piston length	(m)
p	pressure	(N/mm^2)
μ	friction coeffcient	(-)
$F_{2.5}(H_\sigma)$	probability distribution	(-)
X	number of asperities	(-)
β'	asperity radius	(m)
Ω	constant	(-)
h	oil film thickness	(m)
σ	surface roughness	(Rq)
υ	poisson ratio	(-)
τ	lubricant shear pressure	(Pa)
$\Phi_f, \Phi_{fs}, \Phi_{fp}$	shear factors	(-)
$\bar{h}$	mean oil film thickness	(m)
N	crankshaft angular speed	RPM
c	clearance	(m)
Z	total crank bearing length	(m)
r	crankshaft radius	(m)
γ	oil viscosity	(Pa.s)
D	diameter	(m)
R	diameter	(m)

Subscript

f	friction
ls	lubricant shear
B	bearing
k	thrust bearing
0	inner
1	outer

REFERENCES

Cetin et al. (2014) Appliance Daily Energy Use in New Residential Buildings: Use Profiles and variation in time-of-use, *Energy and Buildings*, 84, (716-726).

Greenwood, J. A., and Tripp, J. H. (1971), The Contact of Two Nominally Flat Rough Surfaces, *Proc. Inst. Mech. Eng*., 185, 625–633.

Greenwood, J. A. and Williamson J. B. P. (1966) Contact of Nominally Flat Surfaces, *Proceedings of Royal Society of London, Series A, Mathematical and Physical Sciences*, 295-1442, 300-319.

Gunelsu, O., and Akalin, O. (2014). The Effects of Piston Skirt Profiles on Secondary Motion and Friction. *J. Eng. Gas Turbines Power*. 136(6): 062503.

Hu, Y., Cheng, H. S., Arai, T., Kobayashi, Y., and Aoyama, S. (1994). Numerical Simulation of Piston Ring in Mixed Lubrication-A Nonaxisymmetrical Analysis. *J. Tribol*., 116(3): 470–478

Jedynak R., and Gilewicz J. (2013), Approximation of the Integrals of the Gaussian Distribution of Asperity Heights in the Greenwood-Tripp Contact Model of Two Rough Surfaces Revisited, *Journal of Applied Mathematics*.

Jia B., Mikalsen, R., Smallbone A., Roskilly A.P., (2018), A study and comparison of frictional losses in free-piston engine and crankshaft engines, *Applied Thermal Engineering*, 140, 217-224.

Kerpicci H., Sahin C., Ozdemir A.R., (2019), A New Approach to Mechanical Loss Measurement of a Reciprocating Compressor, *IOP Conf Ser: Mater Sci. Eng.* 604(1):012057.

Mantri, P., Tamma, B., Kachhia B., Bhakta, A., (2014), Parametric Study of Friction Model for a Reciprocating Compressor, *International Compressor Engineering Conference,* Paper 1151.

Nagata S. Kousokabe, H., Sekiyama, N., Uno, T., (2012), A Low friction thrust bearing for reciprocating compressors. *International Compressor Engineering Conference.* Paper 1160.

Patir, N., and Cheng, H. S., (1978). An Average Flow Model for Determining Effects of Three-Dimensional Roughness on Partial Hydrodynamic Lubrication. *J. of Lubrication Tech*. 100(1): 12–17.

Rao, V.K., Murty, P.S., Reddy, M.S., Sundaresan, S.A., (1996), Study of acceleating torque requirements of a reciprocating compressor, *International Compressor Engineering Conference.* Paper 1083.

R.T. Barrett (1990), Fastener Design Manual, *NASA Reference Publication*-1228.

Zhu, D., Cheng, H. S., Arai, T., and Hamai, K. (1992). A Numerical Analysis for Piston Skirts in Mixed Lubrication—Part I: Basic Modeling. *J. Tribol*. 114(3): 553–562.

ACKNOWLEDGEMENTS

The authors would like to thank the Scientific and Technological Research Council of Turkey (TÜBİTAK) and Arçelik A.Ş. for supporting this research via TÜBİTAK Project Number 118C141.